metals

MDPI

Article

Calculation Model for Activity of FeO in Quaternary Slag System SiO_2-CaO-Al_2O_3-FeO

Zhi Li [1,2,3], Guojun Ma [1,2,3,*], Mengke Liu [1,2,3] and Jingjing Zou [1,2,3]

1 State Key Laboratory of Refractories and Metallurgy, Wuhan University of Science and Technology, Wuhan 430081, China; zhili@wust.edu.cn (Z.L.); liumengke@wust.edu.cn (M.L.); zjj980125@icloud.com (J.Z.)
2 Hubei Provincial Engineering Technology Research Center of Metallurgical Secondary Resources, Wuhan University of Science and Technology, Wuhan 430081, China
3 Key Laboratory for Ferrous Metallurgy and Resources Utilization of Ministry of Education, Wuhan University of Science and Technology, Wuhan 430081, China
* Corresponding author: gma@wust.edu.cn; Tel.: +86-27-68862810

Received: 17 August 2018; Accepted: 6 September 2018; Published: 12 September 2018

Abstract: According to the coexistence theory of slag structure, a calculation model for the activity of FeO in the quaternary system SiO_2-CaO-Al_2O_3-FeO of depleted copper slag was established. The model was used to calculate and analyze the effects of temperature (T), basicity (B), and Al_2O_3 content on the activity of FeO (N_{FeO}). The results show that temperature has little impact on N_{FeO}. With increased basicity, N_{FeO} first increased slightly, then increased sharply, and finally decreased. It is easier for CaO to combine with SiO_2 than FeO to form calcium silicate, which replaces FeO in $2FeO{\cdot}SiO_2$ and increases N_{FeO}. However, when basicity is higher than 2.0, CaO not only reacts with SiO_2, but also combines with FeO to form calcium ferrate compounds to decrease N_{FeO}. In addition, the activity of FeO decreases with increased Al_2O_3 content because of the reaction between CaO and Al_2O_3. The results can be used as a theoretical basis to guide the carbothermal reduction process of copper slag.

Keywords: copper slag; activity of FeO; calculation model for activity

1. Introduction

In the last 50 years, copper consumption has tripled because of rapid industrial development [1]. The production of refined copper was 23.33 Mt in 2016, and the quantity of copper increases year by year [1]. According to a prediction by the International Copper Study Group (ICSG), the global supply of refined copper slightly increased by 0.9% in 2017, far below the average growth rate of 3% in the previous 10 years, due to the fact that the depletion of global mines is more and more serious, and the grade of newly discovered mines is low. Considering the huge consumption and lack of supply, it is extremely urgent to make full use of copper production and other Cu-containing wastes.

Copper slag is one of the byproducts of the copper production process. Typically, about 2.2–3 t of copper slag are generated per ton of matte produced [2,3], which indicates that the annual output of copper slag was at least 51.33 Mt in 2016. There are abundant metals in copper slag, in which the grades of copper and iron are close to or even higher than corresponding ores of copper and iron. There are several main processes of recycling copper and iron in copper slag, such as beneficiation, oxidation-magnetic separation, smelting reduction, and carbothermal reduction at high temperature. It is generally believed that smelting reduction and carbothermal reduction at high temperature are effective ways to reutilize copper slag, which can obtain carbon-saturated molten iron containing less than 0.4% copper [4–7]. Zhang et al. [8] reported on copper slag and iron-bearing slag as flux to recover iron and separate phosphorus, where the recovery of iron could be as high as 90%. According to the

results of Xing et al. [9], temperature has a great effect on the recovery of iron and zinc, but has little effect on the recovery of copper. The recovery of iron and copper can reach 91% and 99%, respectively. However, there is a high level of Cu in the recovered iron-bearing product, and it restricts these products from being used in the steelmaking process. Tang et al. [10] reported that the oxidizing ratio of copper in CuO-$FeCl_2$ can reach 62.5% with an argon flow of 50 mL/min at 973 K, based on the fact that it is easier for Cu to react with Cl than Fe and $CuCl_2$ can be volatilized easily. However, the high cost of the recycling process hinders the recycling of copper slag. Therefore, large amounts of copper slag are simply stockpiled or placed in landfills. The residual elements in copper slag, such as Zn, Pb, and As, are potentially leached with rainwater, resulting in excessive levels of heavy metals in groundwater and spread of small particles of copper slag in the air, causing health hazards for nearby people and animals [11,12]. In order to make full use of copper slag and improve the ratio of recycling, the thermodynamics of the carbothermal reduction of copper slag should be further studied.

As the main iron-containing phase of copper slag is fayalite ($2FeO{\cdot}SiO_2$), the activity of FeO has a significant effect on the reduction process. The activity of FeO in blast furnace slag has been investigated by O'Neill et al. [13], Taniguchi et al. [14], and Aroto et al. [15], and has been shown to have relatively low FeO content (<5 wt. %). Zhang [16] utilized the coexistence theory of slag structure to calculate the activity of FeO in the ternary slag system SiO_2-CaO-FeO, and compared with other studies [17], the results are similar. However, the FeO content in copper slag is higher than that in steel slag. Wang et al. [18] employed the coexistence theory of slag structure for the ternary slag system SiO_2-CaO-FeO to calculate the activity of FeO with different basicity in order to recovery iron in copper slag. However, Al_2O_3 in the slag was ignored during the calculation, which led to errors in the results.

The coexistence theory of slag structure was initially proposed by Chuiko [19] and developed by Zhang [16]. The coexistence theory is based on the relevant phase diagrams, thermodynamic relations, and the law of mass balance of ions and molecules coexisting in molten slag, and establishes some equations to calculate the concentrate of components, by which the activity of components is characterized. The theory has already been used in some slag systems, such as CaO-FeO-Fe_2O_3-SiO_2-Cu_2O and MnO-FeO-SiO_2-Al_2O_3 [20,21].

In this paper, a calculation model for the activity of FeO in the quaternary slag system SiO_2-CaO-Al_2O_3-FeO is established according to the coexistence theory of slag structure, in order to analyze the variation of FeO activity with the effect of temperature (T), basicity (B), and Al_2O_3 content and provide a theoretical basis to guide the carbothermal reduction process of copper slag.

2. Calculation Model of Activity

According to the coexistence theory of slag structure and relevant phase diagrams [22] such as CaO-SiO_2, Al_2O_3-CaO, SiO_2-Al_2O_3, SiO_2-FeO, Al_2O_3-FeO, SiO_2-CaO-Al_2O_3, and SiO_2-CaO-FeO, the structural units were determined at 1573–1773 K, shown in Table 1.

Taking the composition of initial slag as $x_1 = \sum$FeO, $x_2 = \sum$CaO, $x_3 = \sum SiO_2$, and $x_4 = \sum Al_2O_3$, $\sum n$ is the sum of moles of ions and molecules in the slag system; N_i (i represents each structural unit) is the mass action concentration of each structural unit after normalization; and N_1, N_2, N_3, and N_4 are $Fe^{2+} + O^{2-}$, $Ca^{2+} + O^{2-}$, SiO_2, and Al_2O_3, respectively. In these chemical equilibria between structural units (Table 2), k_i is the equilibrium constant, which can be acquired from standard Gibbs free energy (ΔG), T is temperature (K), and R is the gas constant, 8.314 J/(mol·K). Equations (1) to (5) are obtained by the law of mass balance, and Equations (6) to (9) can be deduced based on the mass balance equations and equilibrium constants in Table 2 and Equations (1) to (5).

Table 1. Structural units in the slag system.

Simple Ions	Ca^{2+}, Fe^{2+}, O^{2-}
Complex Molecules	$CaO{\cdot}SiO_2$, $2CaO{\cdot}SiO_2$, $3CaO{\cdot}SiO_2$, $3CaO{\cdot}2SiO_2$, $3Al_2O_3{\cdot}2SiO_2$, $3CaO{\cdot}Al_2O_3$, $12CaO{\cdot}7Al_2O_3$, $CaO{\cdot}2Al_2O_3$, $CaO{\cdot}6Al_2O_3$, $CaO{\cdot}Al_2O_3$, $2FeO{\cdot}SiO_2$, $FeO{\cdot}Al_2O_3$, $CaO{\cdot}Al_2O_3{\cdot}2SiO_2$, $2CaO{\cdot}Al_2O_3{\cdot}SiO_2$, $CaO{\cdot}FeO{\cdot}SiO_2$, Al_2O_3, SiO_2

Table 2. Chemical equilibria of structural units.

$(Ca^{2+} + O^{2-}) + SiO_2 = CaO{\cdot}SiO_2$	$\Delta G^{\theta}_{m1} = -81416 - 10.498T$	$N_5 = k_1N_2N_3$
$2(Ca^{2+} + O^{2-}) + SiO_2 = 2CaO{\cdot}SiO_2$	$\Delta G^{\theta}_{m2} = -160431 + 4.160T$	$N_6 = k_2N_2^2N_3$
$3(Ca^{2+} + O^{2-}) + SiO_2 = 3CaO{\cdot}SiO_2$	$\Delta G^{\theta}_{m3} = -93366 - 23.03T$	$N_7 = k_3N_2^3N_3$
$3(Ca^{2+} + O^{2-}) + 2SiO_2 = 3CaO{\cdot}2SiO_2$	$\Delta G^{\theta}_{m4} = -236973 + 9.63T$	$N_8 = k_4N_2^3N_3^2$
$3Al_2O_3 + 2SiO_2 = 3Al_2O_3{\cdot}2SiO_2$	$\Delta G^{\theta}_{m5} = 8589.9 - 17.39T$	$N_9 = k_5N_3^2N_4^3$
$3(Ca^{2+} + O^{2-}) + Al_2O_3 = 3CaO{\cdot}Al_2O_3$	$\Delta G^{\theta}_{m6} = -17000 - 32.0\ T$	$N_{10} = k_6N_2^3N_4$
$12(Ca^{2+} + O^{2-}) + 7Al_2O_3 = 12CaO{\cdot}7Al_2O_3$	$\Delta G^{\theta}_{m7} = -86100 - 205.1T$	$N_{11} = k_7N_2^{12}N_4^7$
$(Ca^{2+} + O^{2-}) + 2Al_2O_3 = CaO{\cdot}2Al_2O_3$	$\Delta G^{\theta}_{m8} = -16400 - 26.8T$	$N_{12} = k_8N_2N_4^2$
$(Ca^{2+} + O^{2-}) + 6Al_2O_3 = CaO{\cdot}6Al_2O_3$	$\Delta G^{\theta}_{m9} = -17430 - 37.2T$	$N_{13} = k_9N_2N_4^6$
$(Ca^{2+} + O^{2-}) + Al_2O_3 = CaO{\cdot}Al_2O_3$	$\Delta G^{\theta}_{m10} = -18120 - 18.62T$	$N_{14} = k_{10}N_2N_4$
$2(Fe^{2+} + O^{2-}) + SiO_2 = 2FeO{\cdot}SiO_2$	$\Delta G^{\theta}_{m11} = -28596 + 3.349T$	$N_{15} = k_{11}N_1^2N_3$
$(Fe^{2+} + O^{2-}) + Al_2O_3 = FeO{\cdot}Al_2O_3$	$\Delta G^{\theta}_{m12} = -33272.8 + 6.1028T$	$N_{16} = k_{12}N_1N_4$
$(Ca^{2+} + O^{2-}) + Al_2O_3 + 2SiO_2 = CaO{\cdot}Al_2O_3{\cdot}2SiO_2$	$\Delta G^{\theta}_{m13} = 28006 - 74.795T$	$N_{17} = k_{13}N_2N_3^2N_4$
$2(Ca^{2+} + O^{2-}) + Al_2O_3 + SiO_2 = 2CaO{\cdot}Al_2O_3{\cdot}SiO_2$	$\Delta G^{\theta}_{m14} = -17092 + 8.778T$	$N_{18} = k_{14}N_2^2N_3N_4$
$(Ca^{2+} + O^{2-}) + (Fe^{2+} + O^{2-}) + SiO_2 = CaO{\cdot}FeO{\cdot}SiO_2$	$\Delta G^{\theta}_{m15} = -72996.8 - 29.3169T$	$N_{19} = k_{15}N_1N_2N_3$

The ternary phase diagram of SiO_2-CaO-Al_2O_3 is depicted in Figure 1 using FactSage software (Version 7.0, GTT-TECHNOLOGIES, Herzogenrath, Germany). According to the phase diagram, two kinds of slags are suitable to recover iron for less energy consumption, better liquidity, and less viscosity. The major chemical composition of the initial copper slag and the composition of the two kinds of slag are shown in Table 3. Considering high FeO content, the quaternary slag system of SiO_2-CaO-Al_2O_3-FeO has been established.

The activity calculation program was developed based on Equations (6) to (9), the equilibrium constants in Table 2, and the components of slags in Table 3. The equilibrium constants k_i (i = 1–15) were obtained first based on specific temperature and the standard Gibbs free energy. Then, the equilibrium constants and the composition of slags in Table 3 were substituted into Equations (6) to (9), and the contents of the composition in the SiO_2-CaO-Al_2O_3-FeO slag system were calculated. According to the variation of temperature and compositions of slag, the effect of temperature, basicity, and Al_2O_3 content were obtained.

$$\sum_{i=1}^{19} N = 1 \tag{1}$$

$$x_1 = (0.5N_1 + 2N_{15} + N_{16} + N_{19})\sum n \tag{2}$$

$$x_2 = (0.5N_2 + N_5 + 2N_6 + 3N_7 + 3N_8 + 3N_{10} + 12N_{11} + N_{12} + N_{13} + N_{14} + N_{17} + 2N_{18} + N_{19})\sum n \tag{3}$$

$$x_3 = (N_3 + N_5 + N_7 + 2N_8 + 2N_9 + 2N_{15} + 2N_{17} + N_{18} + N_{19})\sum n \tag{4}$$

$$x_4 = (N_4 + 3N_9 + N_{10} + 7N_{11} + 2N_{12} + 6N_{13} + N_{14} + N_{16} + N_{17} + N_{18})\sum n \tag{5}$$

$$\begin{gathered} N_1 + N_2 + N_3 + N_4 + k_1N_2N_3 + k_2N_2^2N_3 + k_3N_2^3N_3 + k_4N_2^3N_3^2 + k_5N_3^2N_4^3 + k_6N_2^3N_4 + k_7N_2^{12}N_4^7 + k_8N_2N_4^2 \\ + k_9N_2N_4^6 + k_{10}N_2N_4 + k_{11}N_1^2N_3 + k_{12}N_1N_4 + k_{13}N_2N_3^2N_4 + k_{14}N_2^2N_3N_4 + k_{15}N_1N_2N_3 = 1 \end{gathered} \tag{6}$$

$$\begin{gathered} x_3\left(0.5N_2 + 3k_6N_2^3N_4 + 12k_7N_2^{12}N_4^7 + k_8N_2N_4^2 + k_9N_2N_4^6 + k_{10}N_2N_4\right) - x_2\left(N_3 + 2k_5N_3^2N_4^3 + k_{11}N_1^2N_3\right) + \\ \left(k_1N_2N_3 + k_5N_3^2N_4^3\right)(x_3 - x_2) + \left(k_2N_2^2N_3 + k_4N_2^3N_3^2\right)(2x_3 - x_2) + k_3N_2^3N_3(3x_3 - x_2) + k_4N_2^3N_3^2(3x_3 - 2x_2) + \\ k_{13}N_2N_3^2N_4(x_3 - 2x_2) = 0 \end{gathered} \tag{7}$$

$$\begin{gathered} x_2\left(N_4 + 3k_5N_3^2N_4^3 + k_{12}N_1N_4\right) - x_4(0.5N_2 + k_1N_2N_3 + 2k_2N_2^2N_3 + 3k_3N_2^3N_3 + 3k_4N_2^3N_3^2 + k_{15}N_1N_2N_3) + \\ k_6N_2^3N_4(x_2 - 3x_4) + k_7N_2^{12}N_4^7(7x_2 - 12x_4) + k_8N_2N_4^2(2x_2 - x_4) + k_9N_2N_4^6(6x_2 - x_4) + \\ \left(k_{10}N_2N_4 + k_{13}N_2N_3^2N_4\right)(x_2 - x_4) + k_{14}N_2^2N_3N_4(x_2 - 2x_4) = 0 \end{gathered} \tag{8}$$

$$\begin{gathered} x_3(0.5N_1 + k_{12}N_1N_4) - x_1(N_3 + k_1N_2N_3k_2N_2^2N_3 + k_3N_2^3N_3 + 2k_4N_2^3N_3^2 + 2k_5N_3^2N_4^3 + 2k_{13}N_2N_3^2N_4 + \\ k_{14}N_2^2N_3N_4) + k_{11}N_1^2N_3(2x_3 - x_1) + k_{15}N_1N_2N_3(x_3 - x_1) = 0 \end{gathered} \tag{9}$$

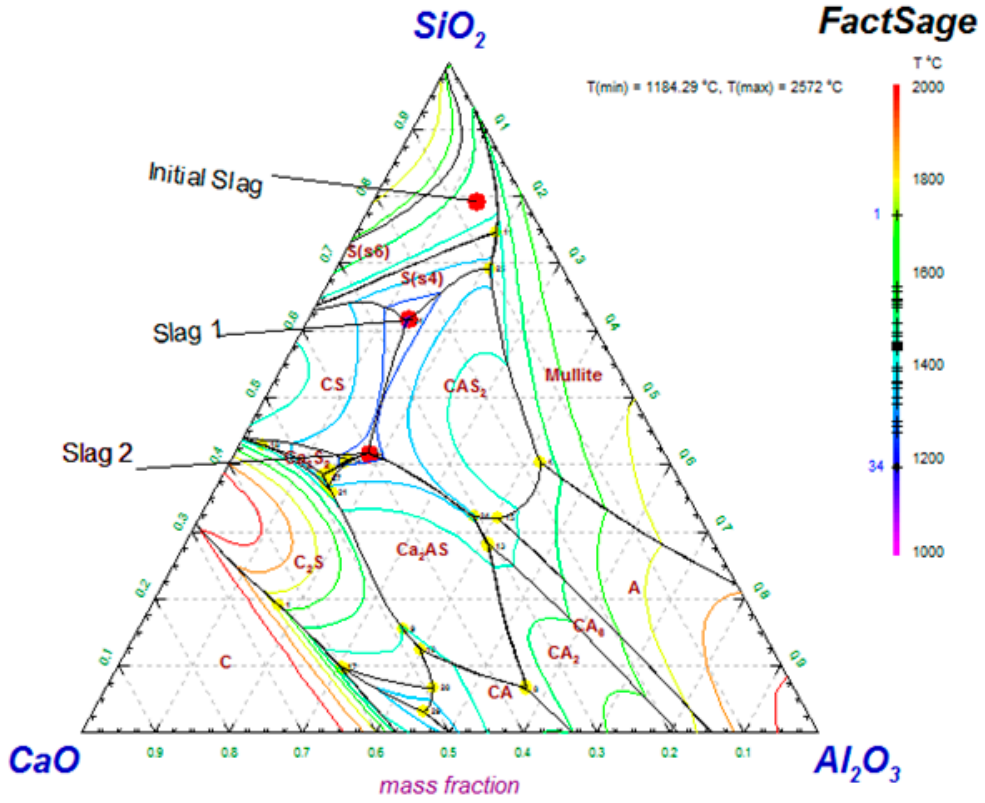

Figure 1. Phase diagram of SiO_2-Al_2O_3-CaO.

Table 3. Chemical composition of copper slag (wt. %).

Slag Type	SiO_2	Al_2O_3	CaO	FeO	R
Initial	39.96	7.21	3.35	49.47	0.08
1	34.91	7.61	14.27	43.22	0.4
2	27.50	11.90	26.55	34.05	0.95

3. Results and Discussion

3.1. Effect of Temperature on Activity of FeO

To consider the effect of temperature on the activity of FeO (N_{FeO}), N_{FeO} was calculated in the different slags shown in Table 3 and at a temperature range of 1573–1823 K. The results are shown in Figure 2. It was found that N_{FeO} in the two slags increased slightly with increased temperature. Figure 3 shows the activity of some components in slag 2 at different temperatures. F, S, C, and A represent FeO, SiO_2, CaO, and Al_2O_3, respectively.

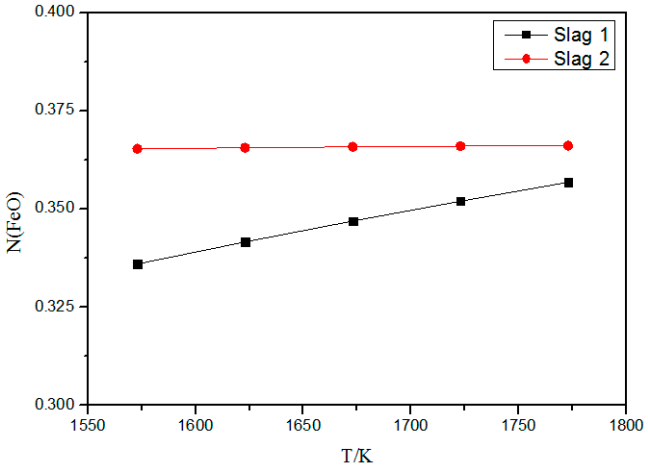

Figure 2. Effect of temperature on activity of FeO.

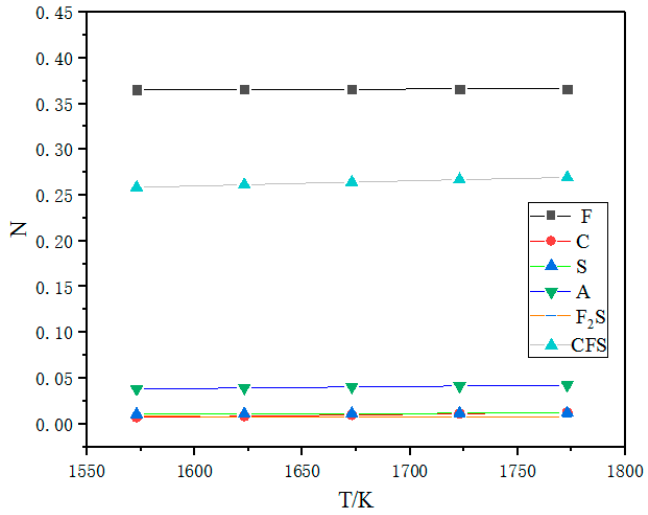

Figure 3. Activity of some components in slag 2 at different temperatures, F_2S and CFS represent $2FeO{\cdot}SiO_2$ and $CaO{\cdot}FeO{\cdot}SiO_2$, respectively.

From Figure 3, it can be seen that temperature had little effect on N_{FeO} in slag 2. With increased temperature, the activity of F_2S ($2FeO{\cdot}SiO_2$) decreased and, on the contrary, the activity of CFS ($CaO{\cdot}FeO{\cdot}SiO_2$) increased. From Table 2, it can be seen that the reaction between FeO and SiO_2 is exothermic, and the reaction generating $CaO{\cdot}FeO{\cdot}SiO_2$ is spontaneous. Namely, the consumption of FeO is reduced by limiting the reaction between FeO and SiO_2, although the reaction generating $CaO{\cdot}FeO{\cdot}SiO_2$ consumes FeO. These cause N_{FeO} to increase slightly.

3.2. Effect of Basicity on Activity of FeO

To calculate the effect of basicity on N_{FeO}, the contents of Al_2O_3 and FeO were kept constant at 7.61% and 43.36% in slag 1, respectively. In slag 2, the contents of Al_2O_3 and FeO were 11.90% and 33.68%, respectively. From Figure 2, it can be seen that temperature had little effect on N_{FeO}, thus the study was carried out at 1723 K, and basicity was used with binary basicity $R = w(CaO)\%/w(SiO_2)\%$. The results are shown in Figure 4, indicating that the tendency of N_{FeO} was the same with different contents of Al_2O_3 and FeO. N_{FeO} first increased slightly, then increased sharply, and finally decreased. In slag 1, the maximum activity was 0.64 at basicity of 1.7, while the maximum was 0.55 in slag 2 with basicity of 2.0. From Table 2, it can be seen that $\sum n$, the sum of moles of ions and molecules in the slag system, decreased because of the reactions between CaO and SiO_2. According to the equation $N_{FeO} = 2x_{FeO}/\sum n$, N_{FeO} would increase as the reactions between CaO and SiO_2 proceed. On the other

hand, FeO would react with CaO, Al_2O_3, or SiO_2, which would decrease the content of FeO. Since these two are opposite factors, the activity of FeO would appear at the maximum value.

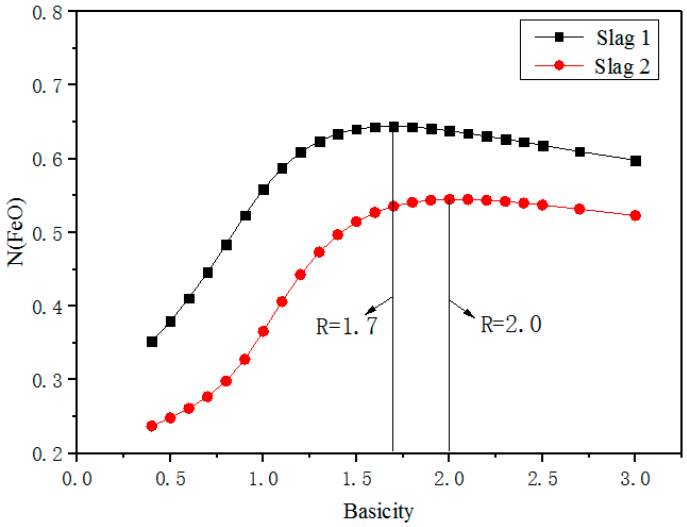

Figure 4. Effect of basicity on N_{FeO}.

In Figure 5, the measured γ_{FeO} results are plotted for slag systems of SiO_2-CaO-Al_2O_3-FeO and SiO_2-CaO-FeO by Taniguchi et al. [14], Arato et al. [15], and Wang et al. [18]. It is found that the present work is in good agreement with the results of Taniguchi et al. and Arato et al., while it is within the wide variation range reported by Wang et al. This is possibly because Al_2O_3 was not considered by Wang et al. Comparing the results of Taniguchi et al., Arato et al., and the present work, the results here are very small, which probably means that the effect of Al_2O_3 on γ_{FeO} is inert in the system.

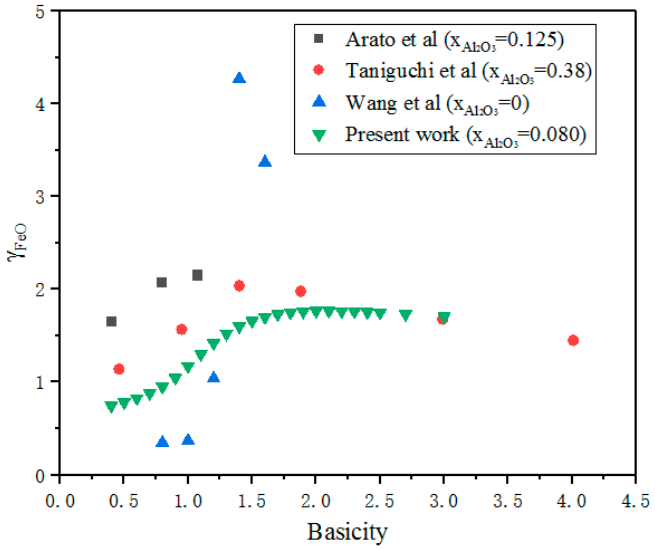

Figure 5. Comparison of present work and reference works.

Figure 6 shows the activity of some components in slag 2 at 1723 K. When basicity was below 0.8, the activity of Al_2O_3 and SiO_2 declined and the activity of CFS ($CaO{\cdot}FeO{\cdot}SiO_2$) increased. As basicity increased to 0.8, there was little activity of $2CaO{\cdot}SiO_2$ and $2FeO{\cdot}SiO_2$ disappeared gradually, which means that CaO reacts with $2FeO{\cdot}SiO_2$ first to form $CaO{\cdot}FeO{\cdot}SiO_2$, instead of forming $2CaO{\cdot}SiO_2$. It proves that while the content of CaO is low, it is hard to replace the FeO from

$2FeO{\cdot}SiO_2$. During the process, $\sum n$ decreased and N_{FeO} increased. Therefore, although the content of FeO decreased, N_{FeO} increased slowly.

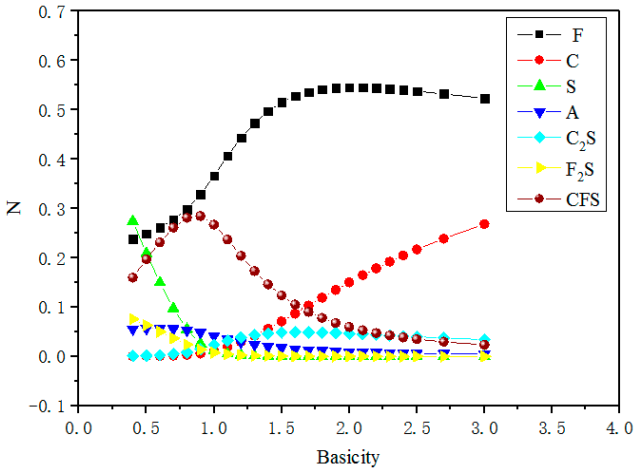

Figure 6. Activity of some components in slag 2 with different basicity, C_2S, F_2S and CFS, represent $2CaO{\cdot}SiO_2$, $2FeO{\cdot}SiO_2$ and $CaO{\cdot}FeO{\cdot}SiO_2$ respectively.

From Figure 6, it can be seen that the tendency of the activity of $2CaO{\cdot}SiO_2$ is same as that of FeO when basicity is higher than 0.8, and the activity of CaO increases while the activity of $CaO{\cdot}FeO{\cdot}SiO_2$ declines. This indicates that CaO reacted with $CaO{\cdot}FeO{\cdot}SiO_2$ to form FeO and $2CaO{\cdot}SiO_2$ with increased basicity, making the activity of FeO and $2CaO{\cdot}SiO_2$ increase. The formation of $2CaO{\cdot}SiO_2$ in copper slag has two steps, shown in Equations (10) and (11): first CaO reacts with $2FeO{\cdot}SiO_2$ to form $CaO{\cdot}FeO{\cdot}SiO_2$ and FeO, and then CaO reacts with $CaO{\cdot}FeO{\cdot}SiO_2$ to form $2CaO{\cdot}SiO_2$ and FeO. CaO is alkaline oxide and can dissociate O^{2-} and Ca^{2+} easily. Meanwhile, CaO has higher alkalinity than FeO. On the contrary, SiO_2 is acidic oxide, which reacts more easily with CaO. FeO bound with SiO_2 in the form of $2FeO{\cdot}SiO_2$ would be free to increase the N_{FeO}.

$$(Ca^{2+} + O^{2-}) + 2FeO{\cdot}SiO_2 = CaO{\cdot}FeO{\cdot}SiO_2 + FeO \quad (10)$$

$$(Ca^{2+} + O^{2-}) + CaO{\cdot}FeO{\cdot}SiO_2 = 2CaO{\cdot}SiO_2 + FeO \quad (11)$$

When basicity reaches near 2.0, maximum N_{FeO} as the affinity of CaO for SiO_2 reaches the maximum value at the ratio of $N_{CaO}/N_{SiO_2} = 2$ [14]. When the value of Si/O is smaller, the structure of silicate is more stable and simpler. With basicity higher than 2.0, the CaO content still increases. By this, all the silicate exists as SiO_4^{4-}, which is the most stable structure (Si/O = 1/4) [23], and O^{2-} cannot continue to be consumed to form silicate. Residual O^{2-} reacts with Fe^{2+} to form FeO_2^-, decreasing the FeO content; in the meantime, residual CaO reacts with FeO to form calcium ferrate compounds. With these two results, the activity of FeO decreases [24].

3.3. Effect of Al_2O_3 on Activity of FeO

N_{FeO} was calculated in different contents of Al_2O_3 for slag 1 and slag 2 with basicity of 1.7 and 2.0, respectively, at 1723 K, as shown in Figure 7. It can be seen that the value of N_{FeO} slightly decreased with increased Al_2O_3 content, but the variation was very small. To study the variation further, the activity of some components in the slag system were calculated and are shown in Figure 8.

From Figure 8, it can be seen that the value of the activity of FA ($FeO{\cdot}Al_2O_3$) is very small, just like the value of the activity of S (SiO_2). Although the activity of $FeO{\cdot}Al_2O_3$ increased with increased Al_2O_3 content, the value of activity of $FeO{\cdot}Al_2O_3$ was so small to be ignored, which means it is hard for Al_2O_3 to react with FeO in this slag system. On the other hand, the activity of $CaO{\cdot}Al_2O_3$ increased, indicating that the Al_2O_3 reacted with CaO and decreased its activity. With such a decrease, it is

difficult for CaO to replace FeO from $2FeO{\cdot}SiO_2$, which decreases the N_{FeO} [24]. CaO can only react with $2FeO{\cdot}SiO_2$ to form $CaO{\cdot}FeO{\cdot}SiO_2$, as in Equation (10). Therefore, the activity of $2CaO{\cdot}SiO_2$ decreases and the activity of $CaO{\cdot}FeO{\cdot}SiO_2$ increases when the content of Al_2O_3 increases.

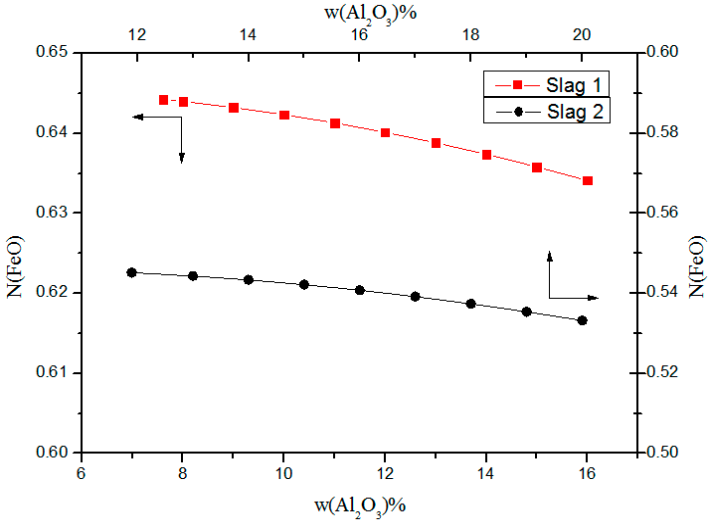

Figure 7. Effect of Al_2O_3 on activity of FeO.

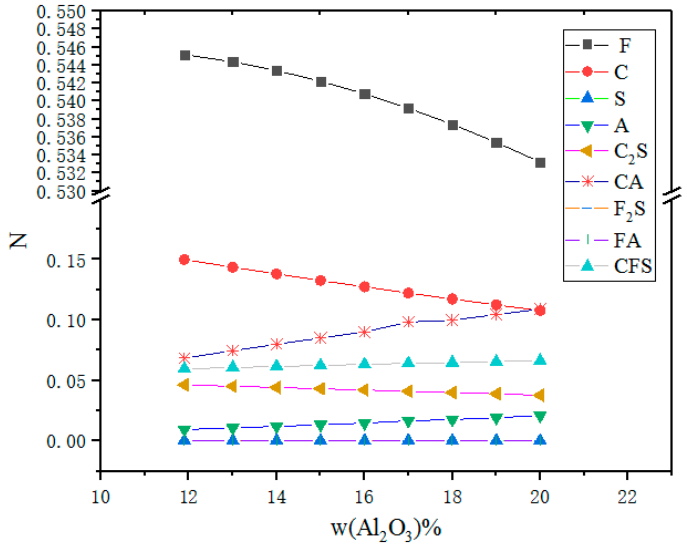

Figure 8. Activity trend of some components in slag 2, C_2S, CA, F_2S, FA and CFS represent $2CaO{\cdot}SiO_2$, $CaO{\cdot}Al_2O_3$, $2FeO{\cdot}SiO_2$, $FeO{\cdot}Al_2O_3$ and $CaO{\cdot}FeO{\cdot}SiO_2$, respectively.

4. Conclusions

1. The calculation model can predict the activity of components generated in the quaternary slag system SiO_2-CaO-Al_2O_3-FeO with different temperatures, basicity, and Al_2O_3 content. Temperature influences the activity of N_{FeO} slightly at 1573–1773 K.
2. Basicity is the major factor affecting the activity of FeO. With basicity ranging from 0.4 to 0.8, N_{FeO} increased slightly due to the formation of $CaO{\cdot}FeO{\cdot}SiO_2$. When basicity reaches near 2.0, there is maximum N_{FeO}, as CaO can react with SiO_2 to form the most stable and simplest structure, SiO_4^{4-} (Si/O = 1/4). When basicity is higher than 2.0, CaO not only reacts with SiO_2, but also combines with FeO to form calcium ferrate compounds to decrease N_{FeO}.
3. The value of N_{FeO} slightly decreases with increased Al_2O_3 content, as CaO reacts with Al_2O_3, which limits the free FeO generated from $2FeO{\cdot}SiO_2$.

Author Contributions: Conceptualization, G.M.; Methodology, Z.L.; Software, Z.L. and M.L.; Validation, Z.L. and G.M.; Formal Analysis, Z.L. and M.L.; Investigation Z.L., M.L. and J.Z.; Resources, Z.L. and G.M.; Data curation, M.L. and J.Z.; Writing-Original Draft Preparation, Z.L.; Writing-Review & Editing, G.M.; Visualization, M.L.; Supervision, G.M.; Project Administration, G.M.; Funding Acquisition, G.M.

Funding: This research was funded by Hubei Provincial Special Project on Technology Innovation (Foreign Scientific and Technological Cooperation), grant number: 2017AHB042.

Conflicts of Interest: The authors declare no conflict of interest.

References

1. The International Copper Study Group (ICSG). The World Copper Factbook 2016. Available online: http://www.icsg.org/index.php?option=com_content&task=view&id=22&itemid=26 (accessed on 5 May 2018).
2. Gorai, B.; Jana, R.K.; Premchand. Characteristics and utilization of copper slag—A review. *Resour. Conserv. Recycl.* **2003**, *39*, 299–313. [CrossRef]
3. Gyurov, S.; Rabadjieva, D.; Kovacheva, D.; Kostova, Y. Kinetics of copper slag oxidation under nonisothermal conditions. *J. Therm. Anal. Calorim.* **2014**, *116*, 945–953. [CrossRef]
4. Sarfo, P.; Young, J.; Ma, G.J.; Young, C. Characterization and recovery of valuables from waste copper smelting slag. In *Advances in Molten Slags, Fluxes, and Salts, Proceedings of the 10th International Conference on Molten Slags, Fluxes and Salts, Seattle, WA, USA, 22–25 May 2016*; Springer International: Cham, Switzerland, 2016; pp. 889–898.
5. Yang, Z.H.; Lin, Q.; Lu, S.C.; He, Y.; Liao, G.D.; Ke, Y. Effect of CaO/SiO_2 ratio on the preparation and crystallization of glass-ceramics from copper slag. *Ceram. Int.* **2014**, *40*, 7297–7305. [CrossRef]
6. Yang, Z.H.; Lin, Q.; Xia, J.X.; He, Y.; Liao, G.D.; Ke, Y. Preparation and crystallization of glass-ceramics derived from iron-rich copper slag. *J. Alloys Compd.* **2013**, *547*, 354–360. [CrossRef]
7. Sarfo, P.; Wyss, G.; Ma, G.J.; Das, A.; Young, C. Carbothermal reduction of copper smelter slag for recycling into pig iron and glass. *Miner. Eng.* **2017**, *107*, 8–19. [CrossRef]
8. Zhang, J.; Dai, X.T.; Yan, D.L.; Qi, Y.H. Carbothermic reduction for collocation use between circulating steelmaking slag and copper slag. *Steels* **2015**, *50*, 114–118.
9. Zhao, K.; Gong, X.R.; Li, J.; Liu, W.X.; Xing, H.W. Thermodynamic of recovering iron, copper, zinc in copper slag by direct reduction method. *J. Environ. Eng.* **2016**, *10*, 2638–2646.
10. Tang, W.D.; Zhu, W.W.; Jiang, P.G.; Jing, Q.X. Kinetics of CuO chlorination process. *Nonferr. Met. Sci. Eng.* **2017**, *8*, 46–50.
11. Cornelis, G.; Johnson, C.A.; Gerven, T.V.; Vandecasteele, C. Leaching mechanisms of oxyanionic metalloid and metal species in alkaline solid wastes: A review. *Appl. Geochem.* **2008**, *23*, 955–976. [CrossRef]
12. Dixit, S.; Hering, J.G. Comparison of arsenic(V) and arsenic(III) sorption onto iron oxide minerals: Implications for arsenic mobility. *Environ. Sci. Technol.* **2003**, *37*, 4182–4189. [CrossRef]
13. O'Neill, H.S.C.; Eggins, S.M. The effect of melt composition on trace element partitioning: An experimental investigation of the activity coefficients of FeO, NiO, CoO, MoO_2 and MoO_3 in silicate melts. *Chem. Geol.* **2002**, *186*, 151–181. [CrossRef]
14. Taniguchi, Y.; Morita, K.; Sano, N. Activities of FeO in $CaO\text{-}Al_2O_3\text{-}SiO_2\text{-}FeO$ and $CaO\text{-}Al_2O_3\text{-}CaF_2\text{-}FeO$ Slags. *ISIJ Int.* **1997**, *37*, 956–961. [CrossRef]
15. Arato, T.; Tokuda, M.; Ohtani, M. Activity measurement of Fe_TO in molten blast furnace type slags by EMF method. *Trans. ISIJ* **1982**, *68*, 2263–2270.
16. Zhang, J. *Computational Thermodynamics of Metallurgical Metals and Solutions*, 1st ed.; Metallurgical Industry Press: Beijing, China, 2007; pp. 307–313, ISBN 9787502441647.
17. Timucin, M.; Morris, A.E. Phase equilibria and thermodynamic studies in the system $CaO\text{-}FeO\text{-}Fe_2O_3\text{-}SiO_2$. *Metall. Trans.* **1970**, *1*, 3193–3201.
18. Wang, H.; Li, L. *Applied Basic Research on the Effective Recovery of Valuable Metals from Copper Slags*, 1st ed.; Science Press: Beijing, China, 2013; pp. 34–36, ISBN 9787030360250.
19. Chuiko, N.M. Chemical bonds and the theory of slag structure. *Metallurgist* **1971**, *19*, 2–22.
20. Wang, J.L.; Zhang, C.F.; Tong, C.R.; Zhang, W.H. Action concentration calculation model for slag system of $CaO\text{-}FeO\text{-}Fe_2O_3\text{-}SiO_2\text{-}Cu_2O$. *J. Cent. South. Univ. Technol.* **2009**, *40*, 282–287.

21. Ma, X.C.; Yu, C.M.; Cheng, G.G.; Zhang, J. Calculation model for the concentration of MnO-FeO-SiO_2-Al_2O_3 slag system. *J. Iron. Steel Res. Int.* **2011**, *23*, 4–7.
22. Eisenhüttenleute, V.D.; Neuschütz, D. *Slag Atlas*, 2nd ed.; Verlag Stahleisen GmbH: Düsseldorf, Germany, 1995; pp. 39–154, ISBN 3514004579.
23. Fu, C.S. *The Principle of Non-Ferrous Metallurgy*, 2nd ed.; Metallurgical Industry Press: Beijing, China, 1993; pp. 35–36, ISBN 9787502411503.
24. Xue, Z.L.; Zou, F.; Xiong, R.; Li, J.L.; Zhu, H.Y. Activity model of FeO in refining slag. *J. Chongqing Univ.* **2015**, *5*, 98–103.